Measuring sub-nm adsorbed water layer thickness and desorption rate using a fused-silica whispering-gallery microresonator

2014 Meas. Sci. Technol. 25 055206

(http://iopscience.iop.org/0957-0233/25/5/055206)

IOP Publishing Measurement Science and Technology
Meas. Sci. Technol. **25** (2014) 055206 (6pp) doi:10.1088/0957-0233/25/5/055206

Measuring sub-nm adsorbed water layer thickness and desorption rate using a fused-silica whispering-gallery microresonator

D Ganta, E B Dale and A T Rosenberger

Department of Physics, Oklahoma State University, Stillwater, OK 74078-3072, USA

E-mail: deepak@okstate.edu

Received 8 October 2013, revised 15 January 2014
Accepted for publication 30 January 2014
Published 8 April 2014

Abstract

We report an optical method for measuring the thickness of the water layer adsorbed onto the surface of a high-Q fused-silica microresonator. Light from a tunable diode laser operating near 1550 nm is coupled into the microresonator to excite whispering-gallery modes (WGMs). By observing thermal distortion or even bistability of the WGM resonances caused by absorption in the water layer, the contribution of that absorption to the total loss is determined. Thereby, the thickness of the water layer is found to be ∼0.1 nm (approximately one monolayer). This method is further extended to measure the desorption rate of the adsorbed water, which is roughly exponential with a decay time of ∼40 h when the fused-silica microresonator is held in a vacuum chamber at low pressure.

Keywords: microresonator, thin films, monolayer, thermal bistability, optical sensor, whispering-gallery modes, gas–surface interactions

(Some figures may appear in colour only in the online journal)

1. Introduction

When fused silica is exposed to atmospheric water vapor, a layer of water is adsorbed onto its surface, where the adsorbate can be investigated through its interaction with an evanescent optical field [1–4]. The evanescent field could be provided, for example, by whispering-gallery modes (WGMs) if the fused-silica material is in the form of a microsphere. WGMs of dielectric microresonators can serve as sensitive probes of their environment, through the environment's interaction with the WGMs' evanescent components. For example, high quality factor (Q) WGM resonances have been used for microcavity-enhanced laser absorption spectroscopy of molecules in the ambient gas or liquid [5, 6]. These high-Q microresonators, with a long photon storage time, are of interest in various applications such as cavity quantum electrodynamics, environmental probes, atom trapping, low threshold lasers, sensing, optical filtering and nonlinear optics [7–13].

In the work reported here, a tapered fiber, tangent to a double-stem microresonator in its equatorial plane, carries light from a tunable diode laser to excite WGMs of the microresonator by optical tunneling when the evanescent fields of the fiber mode and WGM overlap. This coupling fiber is reduced in diameter to 2–3 μm by heating and stretching, using the hydrogen–oxygen torch and the translation stages shown in figure 1. The double-stem microresonator, one example of which is shown in figure 2, is fabricated using the same apparatus, by gently heating the junction of two stripped and cleaned fibers while pushing them together using the translation stages. Surface tension pulls the molten silica into a spheroidal shape with an equatorial radius of a few hundred μm. Both stems are then tapered to diameters of about 3 μm, to minimize heat loss by stem conduction. The two stems are then epoxied to a steel mount shown in figure 1 before the microresonator is removed from the translation stages.

As soon as the double-stem microresonator is fabricated, upon exposure to the atmosphere a layer of water is adsorbed

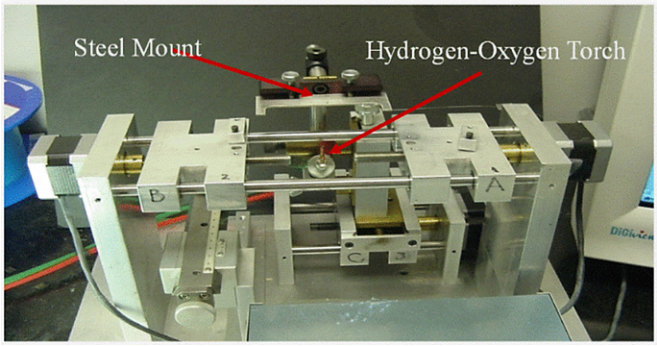

Figure 1. Apparatus used for tapering fiber and fabricating double-stem microresonator.

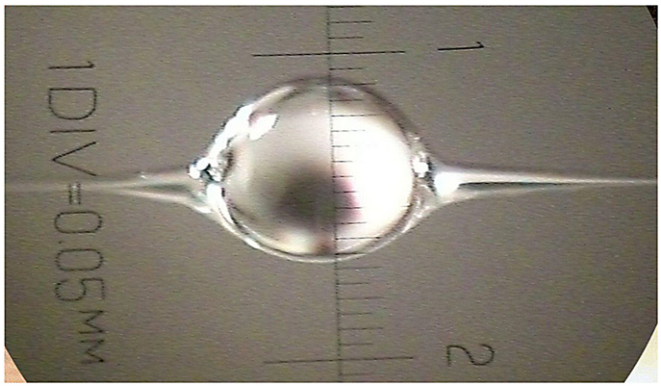

Figure 2. Photograph of a typical fused-silica microsphere with two thin (∼3 μm diameter) stems. This one has an equatorial radius of approximately 300 μm.

onto its surface. The work here is an extension of our earlier measurements [7, 14]. Thermal distortion, leading to bistability if it is large enough, of a WGM resonance is caused by absorption of the circulating light by the surface water layer and subsequent thermorefractive redshift of the resonance frequency. The distorted response gives us the heat supplied by the fraction of total optical power lost due to absorption, and thus can be used to find the contribution of the water film absorption to the total optical loss [14, 15]. This minimally invasive ultrasensitive method can therefore determine the thickness of the sub-nm absorbing layer of water formed at ambient conditions with a precision of a few pm. Performing this thickness measurement at various times after the ambient pressure has been reduced to the mTorr range then allows the determination of the rate of desorption of the water layer.

The properties of water layers on silica have been studied for several decades. The modern literature concentrates on silica films of varied porosity [16–21], from native oxide on Si, to films produced by chemical vapor deposition, to silica nanoparticle aerogels. Methods used for characterizing their adsorbed water include infrared absorption measured by diffuse reflectance [16], laser-induced thermal desorption [17], nuclear magnetic resonance [18], and impedance and capacitive response [19], among others. In contrast to these techniques, our method is simple, precise and non-invasive. Scanning probe methods [20] require a complex setup and proper sample preparation, only provide nm accuracy, and different scanning probe techniques such as distance dynamic force spectroscopy and distance tunneling spectroscopy produce results that do not agree well with each other. Our WGM absorption method has better precision than the WGM frequency-shift method described in [21], and has the further advantage that it is less sensitive to the 1.6 MHz mK^{-1} frequency shift of WGMs in a silica microresonator that results from temperature fluctuations.

2. Theory

A wide range of thermally induced behavior such as hysteretic wavelength response and oscillatory instability is observed experimentally for microsphere WGMs [14, 15, 22, 23]. Thermal distortion refers to a microsphere's throughput signal depending on the laser frequency scan direction. If the power of the laser that excites the WGMs is high enough (∼150 μW in our case), its absorption will heat the microsphere if it is scanned slowly enough across a WGM resonance. When the laser frequency is scanned in the direction of increasing frequency, a fraction of its power is absorbed as it approaches the WGM resonance, thus shifting the WGM frequency downward, opposite to the scan direction. This causes the apparent WGM linewidth to be smaller than its actual linewidth. When the laser frequency is scanned in the direction of decreasing frequency, the resonance frequency redshift results in an apparent linewidth larger than the actual linewidth. When this effect is large enough, it will result in thermal bistability.

By reducing the input power to a level too low to produce any distortion, the characteristics of a WGM can be measured. The throughput power (carried by the fiber after coupling to the WGM) shows a Lorentzian dip as the laser is scanned through a WGM resonance at frequency ν_0. This dip has linewidth $\Delta\nu$ and fractional depth $M_0 = 4x/(1+x)^2$, where $x = |\kappa|^2/2\pi\, a\alpha_i$ is the ratio of coupling loss $|\kappa|^2$ to intrinsic loss $2\pi\, a\alpha_i$, in which a is the microsphere's equatorial radius and α_i is the intrinsic loss coefficient; the (loaded, i.e., with coupling loss included) quality factor is given by

$$Q = \frac{\nu_0}{\Delta\nu} = \frac{2\pi\, n}{\lambda(1+x)\,\alpha_i}, \tag{1}$$

where $n = 1.44$ is the index of refraction of fused silica in the range of wavelengths $\lambda = 1550 \pm 15$ nm. Measurement of ν_0, $\Delta\nu$ and M_0 permits the coupling loss $|\kappa|^2$ and the intrinsic loss coefficient α_i to be found, provided the coupling regime is known [5]. We can determine whether a given WGM is in the undercoupled ($x < 1$) or overcoupled ($x > 1$) regime by observing the throughput response to square-wave input amplitude modulation, as will be discussed in more detail in section 3.

Part of the intrinsic loss is due to surface scattering, and part is due to absorption in the water layer. Other potential contributions to intrinsic loss, such as radiation or silica absorption, are negligible in spheres of this size ($a \sim 400$ μm) at the wavelengths used (∼1550 nm) [2]. By increasing the input power and fitting the observed thermally distorted mode

profiles to the model described below, we can completely specify the system losses, determining the fraction β of the total intrinsic loss that is due to absorption [14, 15]. The effective absorption coefficient is written as

$$\alpha_{\text{abs}} = \beta\alpha_i. \tag{2}$$

If a microsphere is heated to a temperature difference ΔT above room temperature and the heat source is removed, then ΔT will relax exponentially to zero with time constant τ. This time constant depends on the thermal conductivity of the ambient gas and thus on the gas composition and pressure; it also depends on radiative heat loss, but convection is negligible for our small spheres [7]. Implications of this relaxation were discussed in detail in our earlier work [7]. When the microsphere is heated by absorption of the probe laser as it scans through a WGM resonance, the rate of temperature change is modified to include a heating term that depends on the detuning from the temperature-dependent resonance, the depth of the resonance dip and the power incident on the microsphere [14]:

$$\frac{\mathrm{d}\Delta T}{\mathrm{d}t} = \frac{\beta M_0 P_{\text{inc}}}{mc} \frac{\left(\frac{\Delta\nu}{2}\right)^2}{(\nu(t) - \nu_0 + b\Delta T)^2 + \left(\frac{\Delta\nu}{2}\right)^2} - \frac{\Delta T}{\tau}. \tag{3}$$

In equation (3), m is the microsphere mass, c is the specific heat of fused silica, M_0 is the fractional dip depth, P_{inc} is the power incident on the microsphere (and throughput off resonance), $\nu(t)$ is the scanned laser frequency and $\Delta\nu$ is the linewidth of the Lorentzian WGM resonance at $\nu_0 - b\Delta T$ where b is the 1.6 GHz K^{-1} thermorefractive shift. The time constant τ is measured for this microsphere for various ambient gas compositions and pressures in a separate experiment, and so the only free parameter is β, the fraction of the total power loss ($M_0 P_{\text{inc}}$ at maximum) that is due to absorption, as opposed to scattering. Equation (3) gives $\Delta T(t)$ as the laser scans across the WGM resonance, and thus the throughput power as a function of time is given by

$$P_t(t) = P_{\text{inc}}\left(1 - M_0 \frac{\left(\frac{\Delta\nu}{2}\right)^2}{(\nu(t) - \nu_0 + b\Delta T(t))^2 + \left(\frac{\Delta\nu}{2}\right)^2}\right). \tag{4}$$

Now, since we know $\nu(t)$, which is given by the triangle wave that scans the laser frequency up and down at a constant rate, equation (4) can be converted to give $P_t(\nu)$. Fitting the experimental throughput trace to this $P_t(\nu)$ by adjusting the free parameter β gives the value of β, and then the effective absorption coefficient is found from equation (2).

An approximate expression for the relation between the effective absorption coefficient of the water layer α_{abs}, its thickness δ and its bulk absorption coefficient α_b has been given by [2]

$$\delta \cong \left(\frac{\lambda a}{\pi n^5}\right)^{1/2} \frac{\alpha_{abs}}{4\alpha_b}. \tag{5}$$

This assumes that the water layer has the same absorption coefficient as bulk water, but that the effective absorption coefficient is lower because the thin layer occupies only a small fraction of the WGM mode volume. From equation (5) and the value of α_{abs} that is found, we can determine the thickness of an absorbing layer if its bulk absorption coefficient is known, or vice versa.

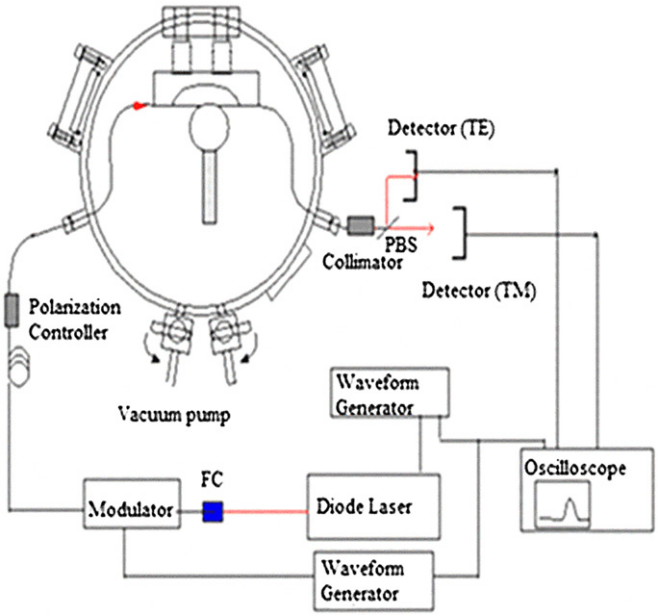

Figure 3. Experimental setup. Light from a frequency-scanned cw diode laser is launched into a bitapered fiber using a FC (fiber-coupler-assembly) to excite WGMs of the microresonator. A polarizing beamsplitter (PBS) separates throughput of the two polarizations and the vacuum chamber allows control over the ambient pressure.

The assumption that layer and bulk water have the same absorption coefficient has been used in earlier work by another group [2]. It is justified by results that show the water film absorption coefficient to be the same, to within about 10%, as that for bulk water, normalized to take their different concentrations into account [24]. Reference [24] gives this near equality for wavelengths near 1.9 μm and also near 6.1 μm, so we assume that it also holds near 1.55 μm.

3. Experimental setup and results

The experimental setup is sketched in figure 3. Light from a cw tunable diode laser (New Focus 6328) is fiber coupled into a lithium niobate Mach–Zehnder amplitude modulator, from which it exits into a single-mode optical fiber that passes through a polarization controller before being fed into a vacuum chamber, where its adiabatic bitapered region is brought into contact with the microsphere. (The vacuum chamber thermally isolates the microsphere from the lab environment; its large mass reduces sensitivity to external temperature fluctuations, and the fact that convection is negligible helps to suppress internal temperature fluctuations.) The diode laser is scanned up and down in frequency by a triangle wave, so that the scan is linear in time and has the same rate in both directions. The modulator is turned on momentarily to determine the coupling regime. Undercoupled and overcoupled WGMs differ qualitatively in their throughput response to square-wave amplitude modulation; an undercoupled WGM will show an overshoot

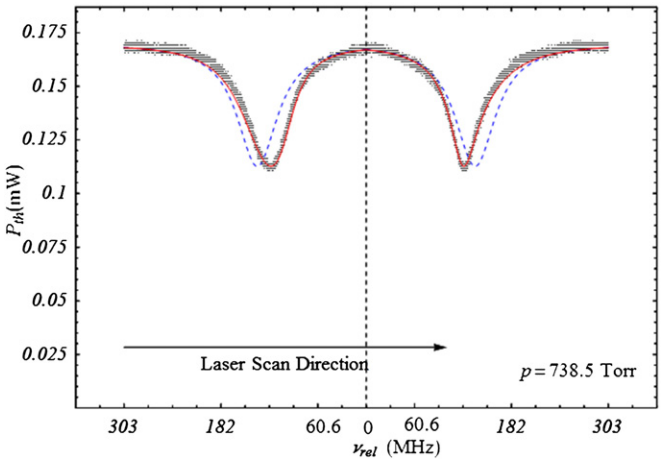

Figure 4. WGM resonance dip showing thermal distortion. The fuzzy black line is experimental data. The red solid line is the theoretical fit. The blue dashed line indicates the mode before distortion (at low power). For this undercoupled mode at $\lambda =$ 1542 nm we have $a = 426$ μm and $Q = 3.16 \times 10^6$. On the left side of the figure, the laser is scanning down in frequency at 6 MHz s^{-1} through the resonance, and on the right the laser scans back up in frequency at the same rate through the same resonance.

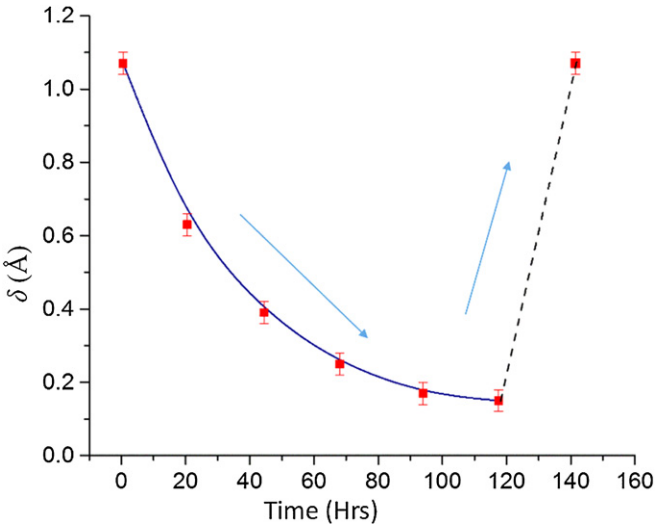

Figure 5. Surface water layer thickness versus time, measured using a microsphere of effective radius 426 μm. The blue line is an exponential fit with a time constant of 43 h. The nitrogen pressure is returned to atmospheric after 120 h, and the subsequent change in thickness is indicated by a dashed line.

at turn-on of the input, before reaching steady state, while an overcoupled WGM will show an initial rise in throughput followed by a drop to zero before rising to steady state. The polarization controller is usually set so that a single WGM eigenpolarization (TE or TM) is excited. Thermal distortion effects are observed in the detected throughput.

Using slow probe laser scan rates ($\sim$10 MHz s^{-1}) and incident power on the order of 150 μW for the microresonators used in our experiments can cause prominent distortion and bistability effects to be observed. We assume that for modes of differing radial order, which will have differing evanescent fractions, the effective absorption constants should be very similar [21] because while the evanescent extent increases somewhat with order, the surface water layer is confined to within at most a few nanometers of the surface, which is but a small fraction of the total evanescent field. Therefore, the overall absorption will be very weakly dependent on the radial order of the WGM.

Prior to investigating thermal distortion of a WGM, such as that shown by the black line in figure 4, experiments are done to characterize it. At low input power, the linewidth ($\Delta\nu$) and dip depth (M_0) (e.g., those of the blue dashed line in figure 4) are measured, and the square-wave input modulation response is used to determine the coupling regime, so that the coupling loss and total intrinsic loss are now known. The thermal relaxation time (τ) is measured, at all ambient pressures to be used, through external heating of the microsphere by momentarily focusing a 532 nm laser beam on it [7]. Then a thermal distortion experiment is done by increasing the input power and recording the throughput trace (black line in figure 4). The distorted throughput trace is then fit to the model (red line in figure 4) given by equation (4). The temperature variation with time as the laser scans up and down in frequency, $\Delta T(t)$, is found by solving equation (3) for an assumed value of β and substituted into equation (4) to get a throughput trace for that value of β. This process is repeated, varying β, until the model trace fits the distorted experimental trace. This value of β then gives the value of α_{abs} by using equation (2), and substituting this into equation (5) gives the value of δ, such as the first point plotted in figure 5. The characterization measurements are performed earlier, so recording of the distorted trace takes only seconds, and the fitting process takes only a few minutes, but need not be done in real time.

This procedure was followed using multiple WGMs in several different microresonators at a number of different pressures from 0.022 to 746.4 Torr, and the results were not only repeatable but also consistent for different input powers. Here we present results near atmospheric pressure (738.5 Torr), where the water layer is expected to be approximately one monolayer. Model fitting of the data in figure 4, which are for a 426 μm radius sphere in air at a wavelength of 1542 nm, gives $\alpha_{abs} = 0.0592$ m^{-1}.

Having determined this effective absorption coefficient, and knowing that the bulk absorption coefficient (α_b) of water at this wavelength is 800 m^{-1} [25], we can find the thickness of the water layer from equation (5). The water layer thickness δ will be given in units of Å (1×10^{-10} m), which is approximately that of one monolayer. Values of δ less than 1 Å indicate that there is only partial water coverage on the sphere's surface [24]. If a sphere has been at atmospheric pressure for a long time, then the adsorbed water will be on the order of one monolayer [2, 3]; this is the case in figure 4, where δ is found to be 1.07 Å, with a precision of a few pm. This uncertainty in δ results from uncertainties in measurement and fitting. The uncertainty in measuring the sphere's radius a is about 1%, and thus the uncertainty in its mass m is about 3%; the uncertainty in determining the intrinsic loss coefficient α_i is about 2%, and the dip depth M_0 can be measured with about 1%

precision. The precision in determining the thermal relaxation time τ is affected by uncertainty in measuring pressure, but in most cases is less than 2% [7]. Combining the uncertainties of these quantities appearing in equations (3) and (5) leads to an estimate of somewhat better than 4% precision in determining the value of δ. (This assumes that the water layer absorption is the same as in bulk, but even if a 10% uncertainty is allowed, our precision in determining δ is only decreased to about 11%, or 11 pm).

This work is further extended to find the rate of water desorption from the surface of a silica microsphere. As seen in figure 5, when a microsphere is kept in the vacuum chamber at a low pressure (e.g., 0.024 Torr of nitrogen), δ decreases exponentially with time. The measured data in figure 5 are fit well by an exponential with a decay time of 43 h. At such low pressures, the desorption rate is independent of the ambient gas; the same rate was found when the residual gas in the vacuum chamber was room air. It appears that only the physisorbed water desorbs at low pressure at room temperature; δ appears to be asymptotically approaching 0.15 Å, representing about 15% surface coverage by chemisorbed water. These results are very sensitive to how the silica surface is prepared as the microsphere is fabricated, but are not inconsistent with much earlier measurements using a different method [26]. In addition, part of the difference between attenuation in bulk water and in adsorbate is due to the difference in strengths of physisorption and chemisorption of water on the silica surface; physisorbed water behaves more like bulk water [21]. The absorption coefficient is slightly higher for very low surface coverage where chemisorption dominates [24], and this may lead to an overestimate of δ in such cases. After 120 h, when δ has reached 0.15 Å, the adsorption time is measured by returning the vacuum chamber to atmospheric pressure with room air; δ reaches 1.07 Å after 9–12 min. If the chamber is refilled to atmospheric pressure with dry nitrogen, it takes on the order of 24 h for δ to reach 1 Å, as seen in figure 5, indicated by a dashed line to reflect that we did not make enough observations to determine the precise time dependence.

4. Conclusion

In conclusion, a thermal WGM profile distortion technique permits the measurement of the effective absorption coefficient, and hence the thickness of a water layer (or other surface film) on a dielectric microresonator. We used it to measure the thickness of a layer of water adsorbed on the surface of a fused-silica microresonator under various ambient conditions. If the thickness of a surface film is known, this technique then also permits the measurement of the absorption coefficient of the film, and it can be applied to films of any refractive index and absorption coefficient, provided only that the film is thin enough. This method has also been further extended to measure the desorption rate of water from the surface of a fused-silica microresonator at low ambient pressure. The precision of these measurements is quite good, so the prospect of using these ultrasensitive techniques for the characterization of other thin-film coatings is promising.

Acknowledgments

Jeromy Rezac, Sarah Bates and Seth Koterba contributed to the initial experiments investigating these effects. The vacuum chamber was constructed by Mike Lucas of the Physics/Chemistry Instrument Shop. This work has been supported by the National Science Foundation (NSF) under Grant Number ECCS-0601362 and by the Oklahoma Center for the Advancement of Science and Technology under Grant Number AR072-066.

References

[1] Aarts I M P, Pipino A C R, Hoefnagels J P M, Kessels W M M and van de Sanden M C M 2005 Quasi-ice monolayer on atomically smooth amorphous SiO_2 at room temperature observed with a high-finesse optical resonator *Phys. Rev. Lett.* **95** 166104

[2] Vernooy D W, Ilchenko V S, Mabuchi H, Streed E W and Kimble H J 1998 High-Q measurements of fused-silica microspheres in the near infrared *Opt. Lett.* **23** 247–9

[3] Gorodetsky M L, Savchenkov A A and Ilchenko V S 1996 Ultimate Q of optical microsphere resonators *Opt. Lett.* **21** 453–5

[4] Asay D B and Kim S H 2005 Evolution of the adsorbed water layer structure on silicon oxide at room temperature *J. Phys. Chem.* B **109** 16760–3

[5] Rosenberger A T 2007 Analysis of whispering-gallery microcavity-enhanced chemical absorption sensors *Opt. Express* **15** 12959–64

[6] Farca G, Shopova S I and Rosenberger A T 2007 Cavity-enhanced laser absorption spectroscopy using microresonator whispering-gallery modes *Opt. Express* **15** 17443–8

[7] Ganta D, Dale E B, Rezac J P and Rosenberger A T 2011 Optical method for measuring thermal accommodation coefficients using a whispering-gallery microresonator *J. Chem. Phys.* **135** 084313

[8] Dale E B, Ganta D, Yu D-J, Flanders B N, Wicksted J P and Rosenberger A T 2011 Spatially localized enhancement of evanescent coupling to whispering-gallery modes at 1550 nm due to surface plasmon resonances of Au nanowires *IEEE J. Sel. Top. Quantum Electron.* **17** 979–84

[9] Vollmer F, Arnold S and Keng D 2008 Single virus detection from the reactive shift of a whispering-gallery mode *Proc. Natl Acad. Sci. USA* **105** 20701–4

[10] Braunstein D, Khazanov A M, Koganov G A and Shuker R 1996 Lowering of threshold conditions for nonlinear effects in a microsphere *Phys. Rev.* A **53** 3565–72

[11] Park Y-S, Cook A K and Wang H 2006 Cavity QED with diamond nanocrystals and silica microspheres *Nano Lett.* **6** 2075–9

[12] Spillane S M, Kippenberg T J and Vahala K J 2002 Ultralow-threshold Raman laser using a spherical dielectric microcavity *Nature* **415** 621–3

[13] Ma Q, Rossmann T and Guo Z 2010 Whispering-gallery mode silica microsensors for cryogenic to room temperature measurement *Meas. Sci. Technol.* **21** 025310

[14] Rosenberger A T, Dale E B, Ganta D and Rezac J P 2008 Investigating properties of surfaces and thin films using microsphere whispering-gallery modes *Proc. SPIE* **6872** 68720U

[15] Rokhsari H, Spillane S M and Vahala K J 2004 Loss characterization in microcavities using the thermal bistability effect *Appl. Phys. Lett.* **85** 3029–31

[16] Burneau A, Barrès O, Gallas J P and Lavalley J C 1990 Comparative study of the surface hydroxyl groups of fumed and precipitated silicas: 2. Characterization by infrared spectroscopy of the interactions with water *Langmuir* **6** 1364–72

[17] Sneh O, Cameron M A and George S M 1996 Adsorption and desorption kinetics of H_2O on a fully hydroxylated SiO_2 surface *Surf. Sci.* **364** 61–78

[18] Burneau A, Lepage J and Maurice G 1997 Porous silica–water interactions: I. Structural and dimensional changes induced by water adsorption *J. Non-Cryst. Solids* **217** 1–10

[19] Wang C-T, Wu C-L, Chen I-C and Huang Y-H 2005 Humidity sensors based on silica nanoparticle aerogel thin films *Sensors Actuators* B **107** 402–10

[20] Opitz A, Scherge M, Ahmed S I-U and Schaefer J A 2007 A comparative investigation of thickness measurements of ultra-thin water films by scanning probe techniques *J. Appl. Phys.* **101** 064310

[21] Ma Q, Huang L, Guo Z and Rossmann T 2010 Spectral shift response of optical whispering-gallery modes due to water vapor adsorption and desorption *Meas. Sci. Technol.* **21** 115206

[22] Carmon T, Yang L and Vahala K J 2004 Dynamical thermal behavior and thermal selfstability of microcavities *Opt. Express* **12** 4742–50

[23] Fomin A E, Gorodetsky M L, Grudinin I S and Ilchenko V S 2005 Nonstationary nonlinear effects in optical microspheres *J. Opt. Soc. Am.* B **22** 459–65

[24] Burneau A and Gallas J-P 1998 Vibrational spectroscopies *The Surface Properties of Silicas* ed A P Legrand (Chichester: Wiley) pp 203–4

[25] Hale G M and Querry M R 1973 Optical constants of water in the 200 nm to 200 μm wavelength region *Appl. Opt.* **12** 555–63

[26] Young G J 1958 Interaction of water vapor with silica surfaces *J. Colloid Sci.* **13** 67–85